

Under these assumptions, the invertibility principle can be expressed in the following way. If (22) is differentiated with respect to r , using (24), (25) and the assumption of constant f , the result after multiplication by σ can be written as

$$\frac{\partial}{\partial r} \left[\frac{1}{r} \frac{\partial(rv)}{\partial r} \right] - \frac{\zeta_{a\theta}}{\sigma} \frac{\partial \sigma}{\partial r} = \sigma \frac{\partial P}{\partial r} \tag{26}$$

Differentiating (23) with respect to r and making use of the thermal wind equation (21), we get

$$-g \frac{\partial \sigma}{\partial r} = \frac{\partial^2 p}{\partial r \partial \theta} = \frac{\partial}{\partial \theta} \left[\frac{f_{loc}}{R} \frac{\partial v}{\partial \theta} \right] \tag{27}$$

(For later reference, the relation between R , σ and the static stability can be shown to be

$$R = g/(\sigma N^2 \theta^2) > 0, \tag{28}$$

N^2 being the static stability expressed as the square of the Brunt-Väisälä or buoyancy frequency.) Using (22) and (27), we can write (26) finally as

$$\boxed{\frac{\partial}{\partial r} \left[\frac{1}{r} \frac{\partial(rv)}{\partial r} \right] + g^{-1} P \frac{\partial}{\partial \theta} \left(\frac{f_{loc}}{R} \frac{\partial v}{\partial \theta} \right) = \sigma \frac{\partial P}{\partial r}} \tag{29}$$

a nonlinear equation which can be solved, for instance by relaxation methods, as described below, for the wind profile $v(r, \theta)$ given the PV distribution $P(r, \theta)$. Note that the *isentropic gradient* of P appears on the right-hand side as a prescribed forcing function.

Together with suitable boundary conditions, and the condition (17a), Eq. (29) expresses the invertibility principle in much the same way as was done in Kleinschmidt's original work. Note that if

$$f_{loc} P > 0, \tag{30}$$

as we shall assume, then Eq. (29) is an elliptic equation, so that the problem is well posed. As is well known, (30), together with (23), also expresses the assumption of static, inertial, and 'symmetric' baroclinic stability previously made in section 1(d) (e.g. Hoskins 1974, with f replaced by f_{loc}). Equation (29) is exact; its simple form is due to the assumption of circular symmetry and the use of isentropic coordinates.

Note further that if we were to make the approximations

$$f_{loc} \approx \zeta_{a\theta} = f, \quad R \approx R_{ref}(\theta), \quad \sigma \approx \sigma_{ref}(\theta) \tag{31}$$

everywhere except when calculating the forcing function $\partial P/\partial r$ from (22), where $R_{ref}(\theta)$ and $\sigma_{ref}(\theta)$ are the reference-state profiles of R and σ , then (29) would simplify to

$$\frac{\partial}{\partial r} \left(\frac{1}{r} \frac{\partial(rv)}{\partial r} \right) + \frac{f^2}{g \sigma_{ref}} \frac{\partial}{\partial \theta} \left(R_{ref}^{-1} \frac{\partial v}{\partial \theta} \right) = \sigma_{ref} \frac{\partial P}{\partial r}, \tag{32}$$

which is the isentropic coordinate version of the usual quasi-geostrophic approximation to (29). The elliptic operator on the left-hand side of (32) is now linear and if, further, σ_{ref} and R_{ref} were constants, then apart from its slightly different r -dependence the operator would be a three-dimensional Laplacian, after suitably rescaling the vertical coordinate according to the Prandtl-Rossby-Burger relation

$$\Delta \theta \sim fL/(Rg\sigma)^{1/2} \quad (\text{cf. } H \sim fL/N) \tag{33a}$$

(e.g. Rossby 1938), where L is the horizontal scale of the flow. For a more accurate scale relation corresponding to (29) we may replace f by $(f_{\text{loc}}P\sigma)^{1/2}$, giving

$$\Delta\theta \sim (f_{\text{loc}}P/Rg)^{1/2}L \quad (\text{cf. } H \sim (f_{\text{loc}}P\sigma)^{1/2}L/N), \quad (33b)$$

which would be relevant near the equator. H and $\Delta\theta$ are respectively the scales in physical, xyz space and in $xy\theta$ space, measuring the vertical penetration of the induced flow structure above or below the location of the IPV anomaly. The relevance of $\Delta\theta$ rather than H in the isentropic coordinate description explains why the square of the Brunt-Väisälä frequency appears in the denominator, rather than the numerator of (28).

We shall call the expressions on the right of (33a) the Rossby heights (in $xy\theta$ and xyz space respectively), and denote them by $\Delta\theta_{\text{Rossby}}$ and H_{Rossby} . As is well known, the concept is complementary to that of the Rossby radius of deformation, which is the horizontal scale L obtained from (33a) when $\Delta\theta$ or H is given. If $\Delta\theta_{\text{Rossby}}$ and H_{Rossby} greatly exceed the corresponding reference-density scale heights $\Delta\theta_{\text{density}}$, H_{density} (the scale heights for variation of σ and ρ respectively), then non-Boussinesq effects are important. Order-of-magnitude relations which cover the whole range of $\Delta\theta$ or H are

$$\Delta\theta \sim \min\{\Delta\theta_{\text{Rossby}}, \Delta\theta_{\text{density}}\} \quad \text{and} \quad H \sim \min\{H_{\text{Rossby}}, H_{\text{density}}\} \quad (33c)$$

for the vertical scales for downward penetration of the induced wind field, and

$$\Delta\theta \sim \max\left\{\Delta\theta_{\text{Rossby}}, \frac{(\Delta\theta_{\text{Rossby}})^2}{\Delta\theta_{\text{density}}}\right\} \quad \text{and} \quad H \sim \max\left\{H_{\text{Rossby}}, \frac{(H_{\text{Rossby}})^2}{H_{\text{density}}}\right\} \quad (33d)$$

for its upward penetration (Rossby, *op. cit.*). These more general scaling rules are related to well-known results in tidal theory.*

The fact that the inverse Laplacian is a smoothing operator should be kept in mind; for instance it is the essential reason why Figs. 4, 6 and 12 look like smoothed versions of Figs. 3, 5 and 11 (see also (44) below). There is an associated *scale effect*, whereby small-scale features of given strength in the IPV field have a relatively weak effect on the velocity field whereas large-scale features have a relatively strong effect. As already mentioned, this is one of the reasons for supposing that coarse-grain IPV distributions are dynamically meaningful. Note that the smoothing takes place in the vertical as well as in the horizontal.

The exact operator appearing in (29) is nonlinear because of the presence of the unknown functions f_{loc} , R and σ (σ appearing on the right-hand side). As Figs. 3, 4, 5, 6, 11 and 12 suggest, this operator very often has the same qualitative character as its approximate counterpart in (32), although it should be remembered that differences near fronts and shear lines can be important (e.g. Hoskins and Bretherton 1972). In many circumstances of interest, (29) may be expected to be soluble iteratively, for given $P(r, \theta)$, having regard to any constraint imposed via (17b). The conceptually simplest albeit not

* The alternatives within braces are the asymptotic forms for large and small $H_{\text{density}}/H_{\text{Rossby}}$, as the case may be, of the more precise expression

$$H = |(2H_{\text{density}})^{-1} \pm \sqrt{(H_{\text{Rossby}})^{-2} + (2H_{\text{density}})^{-2}}|^{-1},$$

the + and - signs corresponding to downward and upward penetration respectively, which arises in the theory of very-low-frequency tidal oscillations of negative equivalent depth (Kato 1966; Lindzen 1966). The problem solved by Rossby (1938) is an approximate version of the same problem; both concern the linear response to a forcing effect of a given horizontal scale L at a given level. A convenient reference is Holton (1975), in which it should be noted that the expression (2.85) corresponds apart from sign convention to minus the square of the expression

$$\sqrt{(H_{\text{Rossby}})^{-2} + (2H_{\text{density}})^{-2}}$$

above, H_{Rossby} being equal to $\sqrt{-gh/N^2}$ in Holton's notation, where h is the equivalent depth.

the most powerful method starts from a solution to (32) as first guess, and then refines the initial approximations (31) by straightforward iteration. Notice carefully how the condition (17a) invoking the reference state has to enter into this process. As soon as a guess for $v(r, \theta)$ has been computed from (29), using the previous guesses for $R(p) = R(r, \theta)$, and $\sigma(r, \theta)$, improved approximations to $R(r, \theta)$ and $\sigma(r, \theta)$ must be derived

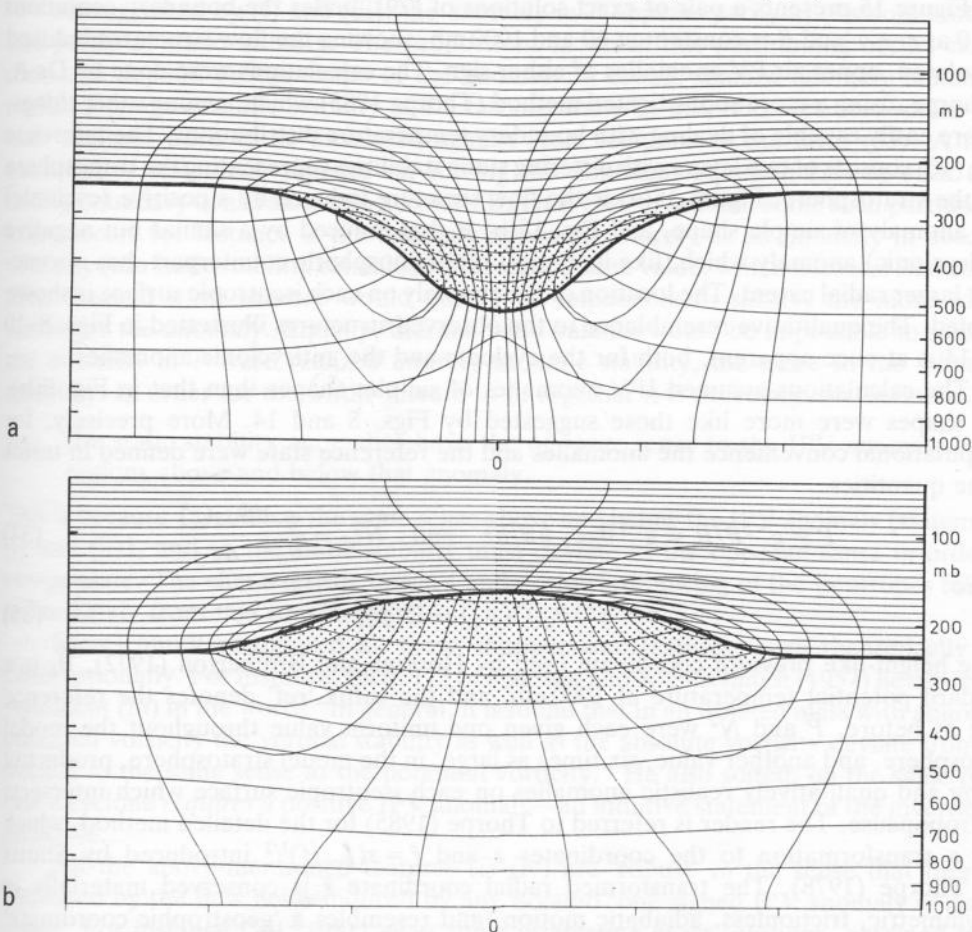


Figure 15. Circularly symmetric flows induced by simple, isolated, IPV anomalies (whose locations are shown stippled) as described in the text. The basic static stability \bar{N} and therefore \bar{P} (defined in (34)) was uniform in the tropospheric region and six times larger in the stratospheric region. The vertical coordinate z is nearly the same as physical height but is defined exactly in (35), g/θ_0 being taken to be $(1/30) \text{ m s}^{-2} \text{ K}^{-1}$. The reference tropospheric 'height' z was 10 km and the total domain 'height' 16.67 km: f was taken to be 10^{-4} s^{-1} . The IPV anomaly was defined by taking the tropopause potential temperature to vary in the manner $\frac{1}{2}A\{\cos(\pi\tilde{r}/r_0) + 1\}$ for $\tilde{r} < r_0$, where $\tilde{r} = r(f_{loc}/f)^{1/2}$. Here the amplitude A was taken to be -24 K in (a) and $+24 \text{ K}$ in (b) which may be compared with a potential temperature increase of 30 K over the depth of the reference troposphere. The parameter r_0 was taken to be 1667 km. The undisturbed θ distribution was imposed as a boundary condition at $\tilde{r} = 5000 \text{ km}$, and the solutions obtained had only a weak dependence of $C_b(\theta)$ upon θ as well as a far-field stratification approximating the reference stratification (16). (In terms of our definitions, the IPV anomaly in the stippled regions must therefore strictly speaking be considered to be embedded in a suitable 'surround' of much weaker anomalies, as noted below (17b).) Only the region $r < 2500 \text{ km}$ is shown here, and the tick marks below the axes are drawn every 833 km. The thick line represents the tropopause and the two sets of thin lines the isentropes every 5 K and the transverse velocity every 3 m s^{-1} . The zero isotach on the axis of symmetry is omitted. In (a) the sense of the azimuthal wind is cyclonic and in (b) it is anticyclonic, in both cases the maximum contour value being 21 m s^{-1} . The surface pressure anomaly is -41 mb in (a) and $+13 \text{ mb}$ in (b) and the relative vorticity extrema (located at the tropopause) are $1.7f$ in (a) and $-0.6f$ in (b). The maximum surface winds are 15 m s^{-1} and 6 m s^{-1} respectively. For more details of the method of computation, see Thorpe (1985).

Courtesy of A. J. Thorpe.

